

## Novel polypyridyl ruthenium(II) complexes containing oxalamidines as ligands

M. Ruben<sup>a</sup>, S. Rau<sup>a</sup>, A. Skirl<sup>a</sup>, K. Krause<sup>a</sup>, H. Görls<sup>a</sup>, D. Walther<sup>a,\*1</sup>, J.G. Vos<sup>b,\*2</sup>

<sup>a</sup> Institut für Anorganische und Analytische Chemie, Friedrich–Schiller-Universität Jena, August-Bebel-Strasse 2, 07743 Jena, Germany

<sup>b</sup> Inorganic Chemistry Research Centre, School of Chemical Sciences, Dublin City University, Dublin 9, Ireland

Received 15 September 1999; accepted 23 November 1999

### Abstract

The complexes [Ru(bpy)<sub>2</sub>(H<sub>2</sub>TPOA)](PF<sub>6</sub>)<sub>2</sub>·4H<sub>2</sub>O (**1**); [Ru(Me-bpy)<sub>2</sub>(H<sub>2</sub>TPOA)](PF<sub>6</sub>)<sub>2</sub>·2H<sub>2</sub>O (**2**); [Ru(bpy)<sub>2</sub>(H<sub>2</sub>TTOA)](PF<sub>6</sub>)<sub>2</sub>·2H<sub>2</sub>O (**3**); [Ru(Me-bpy)<sub>2</sub>(H<sub>2</sub>TTOA)](PF<sub>6</sub>)<sub>2</sub>·2H<sub>2</sub>O (**4**) and {[Ru(bpy)<sub>2</sub>]<sub>2</sub>(TPOA)}(PF<sub>6</sub>)<sub>2</sub>·2H<sub>2</sub>O (**5**) (where bpy is 2,2'-bipyridine; Me-bpy is 4,4'-dimethyl-2,2'-bipyridine; H<sub>2</sub>TPOA is *N,N',N'',N'''*-tetraphenylloxalamidine; H<sub>2</sub>TTOA is *N,N',N'',N'''*-tetratolylloxalamidine) have been synthesised and characterised by <sup>1</sup>H NMR, FAB MS, infrared spectroscopy and elemental analysis. The X-ray investigation shows the coordination of the still protonated oxalamidine moiety via the 1,2-diimine unit. The dimeric compound (**5**) could be separated in its diastereoisomers (**5'**) and (**5''**) by repeated recrystallisation. The diastereomeric forms exhibit different <sup>1</sup>H NMR spectra and slightly shifted electronic spectra. Compared with the model compound [Ru(bpy)<sub>3</sub>]<sup>2+</sup>, the absorption maxima of (**1**)–(**5**) are shifted to lower energies. The mononuclear complexes show Ru(III/II)-couples at about 0.9 V versus SCE, while for the dinuclear complex two well defined metal based redox couples are observed at 0.45 and 0.65 V, indicating substantial interaction between the two metal centres. © 2000 Elsevier Science S.A. All rights reserved.

**Keywords:** Electrochemistry; Ruthenium complexes; Oxalamidines complexes; Polypyridyl complexes

### 1. Introduction

Oligonuclear polypyridyl Ru(II) complexes are being investigated currently in detail because of their rich electrochemical and photophysical properties which render them very attractive systems for modelling electron and energy transfer processes [1], which are known to play a crucial role in biological processes such as respiration, photosynthesis and oxidative DNA cleavage [2].

In most of the compounds described so far, the Ru(II) metal centre is bound to aromatic and polyaromatic pyridyl compounds containing 1,2-diimine units [3]. Less attention has been paid to compounds containing ligands in which the chelating 1,2-diimine unit is

not part of an aromatic system [4] [5]. In this contribution novel ruthenium polypyridyl complexes containing nonaromatic 1,2-diimines are further considered and we report our studies on mono- and dinuclear Ru(II) complexes containing *N,N',N'',N'''*-tetraaryloxalamidines (aryl = phenyl:H<sub>2</sub>TPOA; aryl = tolyl:H<sub>2</sub>TTOA). (For structures of these ligands see Fig. 1.)

The purpose of these investigations is to study the effect that these non-aromatic diimine ligands have on the absorption spectra and the electrochemical properties of ruthenium polypyridyl moieties. Also of interest is the determination of the coordination mode of the ligands. Since oxalamidines can be deprotonated [9], several coordination modes are possible for this type of ligand. The acid–base properties of the ligands can in principle also be used to tune the electronic properties of the ruthenium polypyridyl complexes obtained. The coordination chemistry of these ligands with complex fragments such as Mo(CO)<sub>4</sub>; BR<sub>2</sub> (R = Me); and Cu(I)L has already been reported [6–8].

<sup>1</sup>\*Corresponding author. Tel.: +49-3641-948 100; fax: +49-3641-948 102

<sup>2</sup>\*Corresponding author.

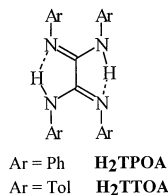


Fig. 1. Structure of the ligands.

## 2. Experimental

### 2.1. Materials

$H_2TPOA$  and  $H_2TTOA$  were prepared according to literature procedures [10].  $RuCl_3 \cdot xH_2O$  was purchased from Strem Chemical and used without further purification. 2,2'-bipyridine and 4,4'-dimethyl-2,2'-bipyridine were obtained from Aldrich.

### 2.2. Instrumentation and measurements

$^1H$  NMR spectra were obtained on a Bruker AC 200 MHz spectrometer and all spectra were referenced to TMS or deuteriated solvent as an internal standard. UV–Vis spectra were recorded on a Shimadzu UV 3100 spectrometer using Teflon stoppered quartz cells having a path length of 1 cm. FAB MS data were obtained on a Finnigan MAT SSQ 710 instrument using 2,4-dimethoxybenzylalcohol as a matrix. Studies of the acid–base properties were carried out in a 50/50% (v:v) mixture of acetonitrile and Britton–Robinson buffer (0.04 M  $H_3BO_3$ ; 0.04 M  $H_3PO_3$ ; 0.04 M  $CH_3COOH$ ). This mixture was used for all measurements and the pH was measured directly with an EDT microprocessor pH-meter calibrated with standard buffers of pH 4.0 and 7.0. The  $pK_a$  constants were obtained from the absorption spectra with the aid of a diagram  $\Delta Abs\%$  versus pH. The electrochemical cell was a conventional three compartment cell. The reference electrode was a saturated calomel electrode and the working electrode was a 3 mm diameter Teflon shrouded glassy carbon electrode and a platinum gauze was used as the counter electrode. A solution of 0.1 M tetraethylammonium perchlorate (TEAP) in acetonitrile was used as the electrolyte in all measurements. Cyclic voltammetry was carried out on a CH-instruments model 660 electrochemical workstation interfaced to an Elonex PC466 personal computer. Analytical HPLC experiments were carried out using a Waters HPLC system, consisting of a model 501 pump, a 20  $\mu$ l injector loop, a Partisil SCX radial PAK cartridge mounted in a radial compression Z module and a Waters 990 photodiode array detector. The system was controlled by a NEC APC III computer. The detection wavelength was 290 nm. The mobile phase used was 90:10  $CH_3CN:H_2O$  containing 0.1 M  $LiClO_4$ . Element-

tal analysis on C, H and N were carried out at the Microanalytical Laboratory of the University College Dublin and at the Friedrich–Schiller-University, Jena.

### 2.3. Preparations

A typical protocol for preparation of compounds **1–4** is as follows (described here for  $[Ru(bpy)_2(H_2TPOA)](PF_6)_2 \cdot 4H_2O$  (**1**)): 0.416 g (0.8 mmol) of  $Ru(bpy)_2Cl_2 \cdot 2H_2O$  were dissolved in 50 ml ethanol–water (95:5 v/v%) and subsequently 0.390 g (1.0 mmol) of  $H_2TPOA$  was added. The mixture was refluxed for 24 h, during which the colour changed from violet to deep red. After cooling to room temperature (r.t.), the solution was evaporated to dryness. The resulting residue was redissolved in a small amount of acetonitrile and purified using column chromatography ( $Al_2O_3$ ; acetonitrile–toluene). The brick red main band was collected and the complex precipitated by adding an excess of aqueous  $NH_4PF_6$ . The precipitate was isolated, washed with diethylether and dried under vacuum. Alternatively, the pure compounds can be also obtained by fractional crystallisation from acetone–water.

$[Ru(bpy)_2(H_2TPOA)](PF_6)_2 \cdot 4H_2O$  (**1**), yield: 84%.  $^1H$  NMR (DMSO- $d_6$ ,  $\delta$ , ppm, 20°C): 10.02 (s, NH, 2H); 9.23 (d,  $H^6$ , 2H), 8.42 (d,  $H^3$ , 2H); 8.24 (t,  $H^4$ , 2H); 8.12 (d,  $H^3$ , 2H); 8.05 (t,  $H^5$ , 2H); 7.71 (t,  $H^4$ , 2H); 7.47 (d,  $H^6$ , 2H), 7.19 (t,  $H^5$ , 2H); 6.96 (t,  $H_{arom}$ , 4H); 6.83 (d,  $H_{arom}$ , 4H); 6.78 (t,  $H_{arom}$ , 2H); 6.56; 6.49; 5.31 (dynamic system,  $H_{arom}$ , 10H). FAB MS (dmbs,  $m/z$ ): 949 ( $[M^+] - PF_6^-$ ); 804 ( $[M^+] - 2PF_6^-$ ). IR [Nujol;  $\nu$ ,  $cm^{-1}$ ]: 3382 (m, NH); 3075 (w, arom. C–H); 1595 (s, C=N); 1448 (s, C=C), 842, 557 (s,  $PF_6^-$ ). UV–Vis (acetonitrile,  $\lambda_{MLCT}$ , nm): 469 ( $\epsilon = 13938$  l  $cm^{-1}$  mol $^{-1}$ ). CV (acetonitrile, 0.1 M TEAP versus SCE,  $E_{Ru(III/II),V}$ ): 0.94; Anal. Calc. C, 48.89; H, 3.75; N, 9.92. Found: C, 48.49; H, 3.95; N, 9.88%.

$[Ru(Me-bpy)_2(H_2TPOA)](PF_6)_2 \cdot 2H_2O$  (**2**), yield: 75%.  $^1H$  NMR (DMSO- $d_6$ ,  $\delta$ , ppm, 20°C): 9.98 (s, NH, 2H); 9.32 (d,  $H^6$ , 2H), 8.42 (d,  $H^3$ , 2H); 8.11 (d,  $H^3$ , 2H); 7.96 (t,  $H^5$ , 2H); 7.54 (d,  $H^6$ , 2H), 7.14 (t,  $H^5$ , 2H); 7.00 (t,  $H_{arom}$ , 2H); 6.99 (t,  $H_{arom}$ , 4H); 6.79 (d,  $H_{arom}$ , 4H); 6.57; 6.45; 5.37 (dynamic system,  $H_{arom}$ , 10H); 2.69 (s,  $CH_3$ , 6H); 2.34 (s,  $CH_3$ , 6H). FAB MS (dmbs,  $m/z$ ): 1005 ( $[M^+] - PF_6^-$ ); 859 ( $[M^+] - 2PF_6^- - H^+$ ). IR [Nujol;  $\nu$ ,  $cm^{-1}$ ]: 3367 (m, NH); 3060 (w, arom. C–H); 2924 (w, C–H); 1619 (s, C=N); 1450 (s, C=C), 845, 558 (s,  $PF_6^-$ ). UV–Vis (acetonitrile,  $\lambda_{MLCT}$ , nm): 476 ( $\epsilon = 11728$  l  $cm^{-1}$  mol $^{-1}$ ). CV (acetonitrile, 0.1 M TEAP versus SCE,  $E_{Ru(III/II),V}$ ): 0.90; Anal. Calc. C, 52.20; H, 4.03; N 9.78. Found: C, 51.88; H, 4.92; N, 8.74%.

$[Ru(bpy)_2(H_2TTOA)](PF_6)_2 \cdot 2H_2O$  (**3**), yield: 72%.  $^1H$  NMR (DMSO- $d_6$ ,  $\delta$ , ppm, 20°C): 9.95 (s, NH, 2H); 9.35 (d,  $H^6$ , 2H), 8.36 (d,  $H^3$ , 2H); 8.09 (m,  $H^4$  u.  $H^3$ , 4H); 7.98 (t,  $H^5$ , 2H); 7.60 (t,  $H^4$ , 2H); 7.43 (d,  $H^6$ ,

2H), 7.08 (t, H<sup>5'</sup>, 2H); 6.57 (dd, H<sub>arom</sub>, 8H); 6.08; 5.49; (dynamic system, H<sub>arom</sub>, 8H); 2.00 (s, CH<sub>3</sub>, 6H); 1.80 (s, CH<sub>3</sub>, 6H). FAB MS (dmbs, *m/z*): 1006 ([M<sup>+</sup>] – PF<sub>6</sub><sup>–</sup> + H<sup>+</sup>); 860 ([M<sup>+</sup>] – 2PF<sub>6</sub><sup>–</sup>). IR (Nujol;  $\nu$ , cm<sup>–1</sup>): 3366 (m, NH); 2923 (w, C–H); 1593 (s, C=N); 1463 (s, C=C), 841, 557 (s, PF<sub>6</sub><sup>–</sup>). CV (acetonitrile, 0.1 M TEAP versus SCE,  $E_{\text{Ru(III/II),V}}$ ): 0.96. UV–Vis (acetonitrile,  $\lambda_{\text{MLCT}}$ , nm): 472 ( $\epsilon = 11274 \text{ l cm}^{-1} \text{ mol}^{-1}$ ); *Anal. Calc.* C, 50.42; H, 4.25; N, 9.44. Found: C, 50.91; H, 4.94; N, 8.66%.

[Ru(Me-bpy)<sub>2</sub>(H<sub>2</sub>TTOA)](PF<sub>6</sub>)<sub>2</sub>·2H<sub>2</sub>O (**4**), yield: 45%. <sup>1</sup>H NMR (DMSO-d<sub>6</sub>,  $\delta$ , ppm, 20°C): 9.56 (s, NH, 2H); 8.96 (d, H<sup>6</sup>, 2H), 8.23 (d, H<sup>3</sup>, 2H); 7.98 (d, H<sup>3'</sup>, 2H); 7.85 (t, H<sup>5</sup>, 2H); 7.18 (d, H<sup>6'</sup>, 2H), 7.05 (t, H<sup>5'</sup>, 2H); 6.80 (dd, H<sub>arom</sub>, 8H); 6.40 (dynamic system, m, H<sub>arom</sub>, 8H); 2.62 (s, CH<sub>3</sub>, 6H); 2.26 (s, CH<sub>3</sub>, 6H); 2.06 (s, CH<sub>3</sub>, 6H); 1.93 (s, CH<sub>3</sub>, 6H). FAB MS (dmbs, *m/z*): 1061 ([M<sup>+</sup>] – PF<sub>6</sub><sup>–</sup> + H<sup>+</sup>); 1004 ([M<sup>+</sup>] – 2PF<sub>6</sub><sup>–</sup> – 3F<sup>–</sup>); 915 ([M<sup>+</sup>] – 2PF<sub>6</sub><sup>–</sup> – H<sup>+</sup>). IR (Nujol;  $\nu$ , cm<sup>–1</sup>): 3371 (m, NH); 3029 (w, arom. C–H); 2924 (w, C–H); 1618 (s, C=N); 1450 (s, C=C), 845, 558 (s, PF<sub>6</sub><sup>–</sup>). CV (acetonitrile, 0.1 M TEAP versus SCE,  $E_{\text{Ru(III/II),V}}$ ): 0.87. UV–Vis (acetonitrile,  $\lambda_{\text{MLCT}}$ , nm): 478 ( $\epsilon = 13983 \text{ l cm}^{-1} \text{ mol}^{-1}$ ); *Anal. Calc.* C, 53.78; H, 4.51; N, 9.29. Found: C, 54.60; H, 4.68; N, 8.76%.

#### 2.4. Preparation of {[Ru(bpy)<sub>2</sub>](TPOA)}(PF<sub>6</sub>)<sub>2</sub>·2H<sub>2</sub>O (**5**)

A total of 195 mg (0.5 mmol) of TPOA were dissolved in 60 ml ethanol–water (50:50 v/v%). An excess of 0.671 g (0.8 mmol) of Ru(bpy)<sub>2</sub>Cl<sub>2</sub>·2H<sub>2</sub>O was added and the resulting solution was refluxed for 8 h. The reaction mixture was treated with an excess of aqueous NH<sub>4</sub>PF<sub>6</sub>. The precipitate was redissolved in acetone–water and pure and mixed fractions of the *meso*-( $\Delta\Delta$ )-compound and the unresolved ( $\Delta\Delta/\Delta\Delta$ ) enantiomeric pair (**5'** and **5''**) could be isolated subsequently by fractional crystallisation. Yield: 1.3 g (84%) of (**5'** and **5''**).

(**5'**): <sup>1</sup>H NMR (DMSO-d<sub>6</sub>,  $\delta$ , ppm, 20°C): 8.78 (d, H<sup>6</sup>, 4H); 8.71 (d, H<sup>3</sup>, 4H); 8.56 (d, H<sup>3'</sup>, 4H); 8.18 (t, H<sup>4</sup>, 4H); 7.77 (t, H<sup>4'</sup>, 4H); 7.69 (t, H<sup>5</sup>, 4H); 7.30 (d, H<sup>6'</sup>, 4H); 7.14 (t, H<sup>5'</sup>, 4H); 6.68 (t, H<sub>arom</sub>, 4H); 6.53 (t, H<sub>arom</sub>, 8H); 5.97 (d, H<sub>arom</sub>, 8H). IR (Nujol;  $\nu$ , cm<sup>–1</sup>): 3036 (w, arom. C–H); 1592 (s, C=N); 1489, 1444 (s, C=C); 842, 557 (PF<sub>6</sub><sup>–</sup>). UV–Vis (acetonitrile,  $\lambda_{\text{MLCT}}$ , nm): 520. CV (acetonitrile, 0.1 M TEAP versus SCE,  $E_{\text{Ru(III/II),V}}$ ): 0.45; 0.64; *Anal. Calc.* C, 51.43; H, 3.66; N, 10.91. Found: C, 52.23; H, 3.42; N, 10.90%.

(**5''**): <sup>1</sup>H NMR (DMSO-d<sub>6</sub>,  $\delta$ , ppm, 20°C): 9.09 (d, H<sup>6</sup>, 4H); 8.90 (d, H<sup>3</sup>, 4H); 8.68 (d, H<sup>3'</sup>, 4H); 8.41 (t, H<sup>4</sup>, 4H); 8.12 (t, H<sup>5</sup>, 4H); 7.80 (t, H<sup>4'</sup>, 4H); 7.29 (d, H<sup>6'</sup>, 4H); 7.13 (t, H<sup>5'</sup>, 4H); 6.41 (t, H<sub>arom</sub>, 4H); 6.09 (t, H<sub>arom</sub>, 8H); 5.70 (d, H<sub>arom</sub>, 8H). IR (Nujol;  $\nu$ , cm<sup>–1</sup>): 3036 (w, arom. C–H); 1592 (s, C=N); 1489, 1444 (s, C=C); 842,

557 (PF<sub>6</sub><sup>–</sup>). UV–Vis (acetonitrile,  $\lambda_{\text{MLCT}}$ , nm): 526. CV (acetonitrile, 0.1 M TEAP versus SCE,  $E_{\text{Ru(III/II),V}}$ ): 0.46; 0.65; *Anal. Calc.* C, 51.43; H, 3.66; N, 10.91. Found: C, 52.87; H, 3.98; N, 10.84%.

#### 2.5. Crystal structure determination of [(bpy)<sub>2</sub>Ru(H<sub>2</sub>TPOA)](PF<sub>6</sub>)<sub>2</sub>·4H<sub>2</sub>O (**1**)

X-ray diffraction was carried out on a Nonius Kappa CCD diffractometer, using graphite-monochromated Mo K $\alpha$  radiation and  $\phi$ -scan technique ( $\Delta\phi = 1^\circ$ , scan-range 180°, time/frame = 30 s) at 20°C. Data were corrected for Lorentz and polarisation effects, but not for absorption [13].

The structure was solved by direct methods (SHELXS [14]) and refined by full-matrix least-squares techniques against  $F^2$  (SHELXL-93 [15]). The hydrogen atoms (without the water molecules) were located by difference Fourier synthesis and refined isotropically. All non-hydrogen atoms were refined anisotropically. XP (Siemens Analytical X-ray Instruments, Inc.) was used for structure representations.

### 3. Results and discussion

#### 3.1. Synthesis and structure of mononuclear complexes **1–4**

The synthesis of ruthenium oxalamidine compounds was accomplished using standard methods. The nuclearity of resulting complexes could be governed by controlling the metal to ligand ratio (see Fig. 2). Nevertheless, in the case of the mononuclear compounds **1–4** some dimer formation could not be prevented and subsequently cleaning by column chromatography was necessary. The <sup>1</sup>H NMR spectra do exhibit the expected pattern of the bpy protons in a C<sub>2</sub>-symmetric Ru(bpy)<sub>2</sub> environment. All protons of the bipyridine ligands could be attributed unambiguously by <sup>1</sup>H–<sup>1</sup>H-COSY experiments.

The signals that can be attributed to the aromatic substituents of the coordinated oxalamidine ligands are found at a higher field than the bipyridine protons. At r.t., only half of the expected aromatic signals for **1–4** are well resolved peaks (see for example compound **3** in Fig. 3). Thus, compound **3** shows for half of the tolyl protons at r.t. one well resolved AA'BB' spin system, while the other half is observed as a broadened signal at about 6.0 ppm. Upon heating, this signal becomes the expected AA'MM' spin system at 5.49 and 6.08 ppm. This dynamic process is most likely explained by hindered rotation of the aryl substituents on the oxalamidine ligands. Interestingly, this behaviour is not observed in the binuclear compound **5** (vide infra). This can be explained by enhanced crowding around the

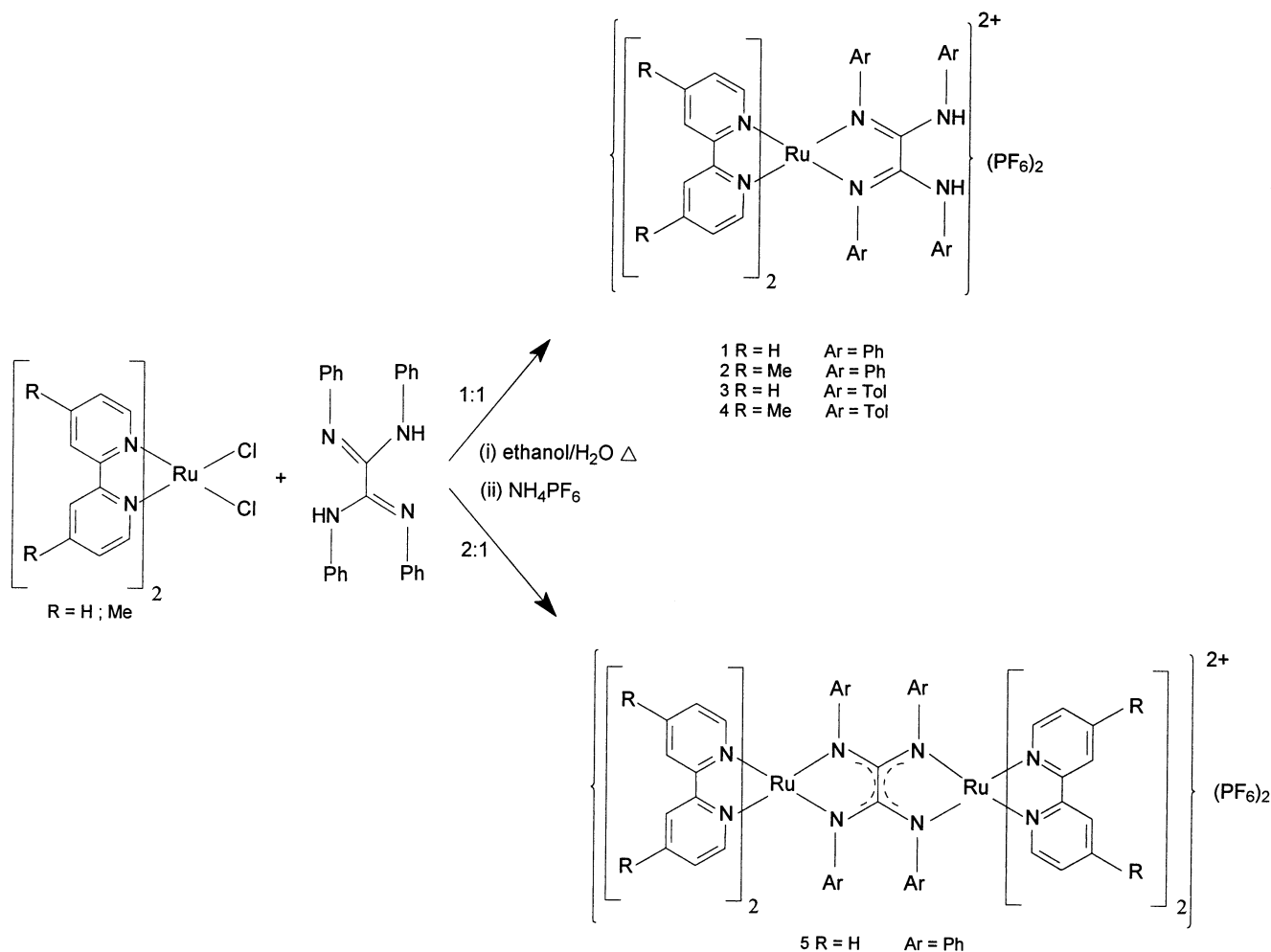


Fig. 2. Synthesis of mononuclear complexes 1–4 and dimeric complex 5.

tetraphenylloxalamidine bridging ligand, not allowing for any rotation of the aryl substituents around the C–N bond.

An important aspect of this study is establishing the coordination mode of the oxalamidine ligand. The tridentate nature of these ligands allows different coordination modes (see Fig. 4) and possible deprotonation of the ligands also needs to be considered.

The presence of protonated secondary amino functions in the mononuclear complexes 1–4 was established from  $^1\text{H}$  NMR measurements, by infrared spectroscopy and by elemental analysis. This protonation behaviour is contrary to that of triazole ligands, where a secondary N–H function is being deprotonated upon coordination [11]. The composition of compounds 1–4 was further confirmed by FAB MS, in which the complexes exhibit characteristic losses of the only electrostatically bound  $\text{PF}_6^-$  anions rendering the cationic complex fragment as the most intense signal (see Section 2).

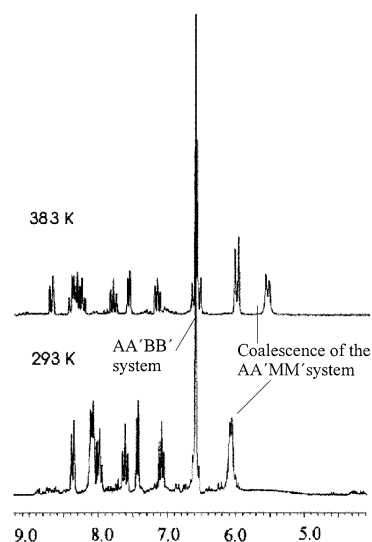


Fig. 3.  $^1\text{H}$  NMR spectra of  $[(\text{bpy})_2\text{Ru}(\text{H}_2\text{TTOA})](\text{PF}_6)_2 \cdot 2\text{H}_2\text{O}$  (3), at 293 and 383 K exhibiting the dynamic behaviour of the aromatic protons of the tetraphenylloxalamidine.

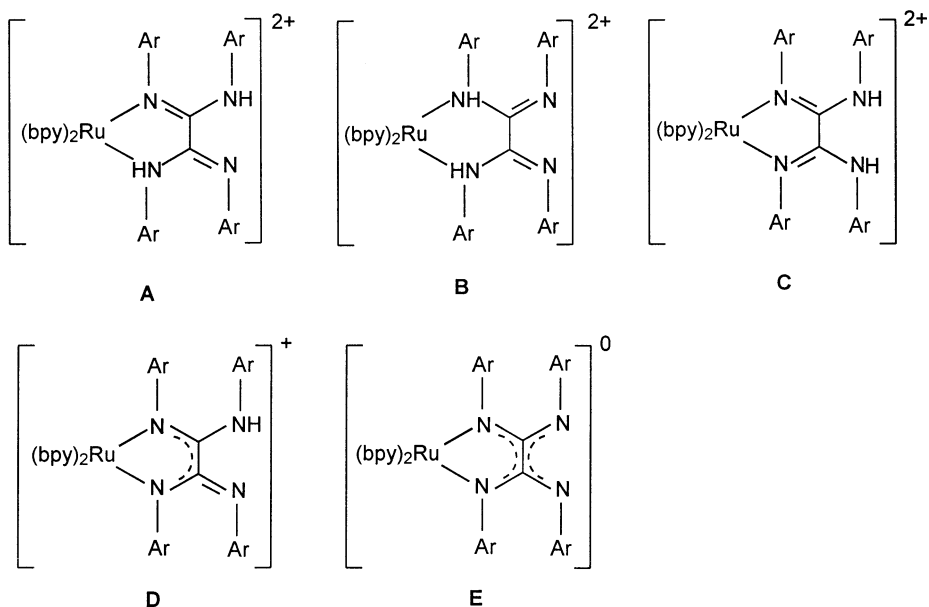


Fig. 4. Possible coordination modes of the oxalamidine ligand towards the  $\text{Ru}(\text{bpy})_2$  moiety.

In order to establish the coordination mode of the ligand, the X-ray structure of complex **1** was determined. Some relevant distances and angles are given in Table 1. As in solution, complex **1** exhibits  $C_2$ -symmetry in the solid state. The result of the X-ray investigations depicted in Fig. 5 demonstrates clearly octahedral coordination of the Ru(II) ion by two bipyridine ligands and by one  $\text{H}_2\text{TPOA}$  ligand. The latter ligand is coordinated via the 1,2-diimine unit. The secondary amines are clearly protonated. The C–N(H) bond length ( $d_{\text{C-N}} = 1.355(5)$  Å) reveals a partial double bond character probably due to the delocalisation of the double bond in the amidine system, but the 1,2-diimine unit is defined clearly by its significantly shorter C–N distance ( $d_{\text{C-N}} = 1.294(4)$  Å). This allows one to draw the unambiguous conclusion, that the tetraphenylloxalamidine is coordinated via its 1,2-diimine system (C in Fig. 4). It is worth emphasising that  $\text{H}_2\text{TPOA}$  is bonded in its *s-cis* configuration while the free ligand exists in crystal form only, as a *s-trans* conformer [12].

The Ru–N(bpy)-distances ( $d_{\text{Ru-N}} = 2.049(3)$ – $2.053(3)$  Å) are in the typical range of other members of the  $\text{Ru}(\text{bpy})_2$  (LL)-class [2], while the Ru–N(oxalamidine) distances are elongated slightly ( $d_{\text{Ru-N}} = 2.081(3)$  Å) indicating the weaker back bonding character of the oxalamidine ligand or maybe a steric hindrance by the phenyl groups. Interestingly the Ru–N distance in the, also neutral, dihydrazone type ligands are significantly shorter at 2.01 Å [4]. The N–Ru–N bite angles show the anticipated values ( $\alpha = 78.7(1)^\circ$ ) for the bipyridines, while the bite angle of the oxalamidine do not exceed  $\alpha = 75.4(2)^\circ$  due to easier pinching of the non rigid oxalamidine system.

In addition, the X-ray investigations reveal intermolecular interactions. In the crystalline state compound **1** forms a polymeric chain of alternating ordered

Table 1  
Selected bond lengths (Å) and angles ( $^\circ$ ) for  $[\text{Ru}(\text{bpy})_2(\text{H}_2\text{TPOA})](\text{PF}_6)_2 \cdot 4\text{H}_2\text{O}$  (**1**)

Ru–N(4)	2.049(3)	N(4)–Ru–N(4A)	173.8(2)
Ru–N(3)	2.053(3)	N(4)–Ru–N(3A)	97.0(1)
Ru–N(1)	2.081(3)	N(4)–Ru–N(3)	78.7(1)
N(1)–C(1)	1.294(4)	N(3A)–Ru–N(3)	91.6(2)
N(2)–C(1)	1.355(5)	N(4)–Ru–N(1)	85.7(1)
C(1)–C(1A)	1.503(6)	N(4A)–Ru–N(1)	99.3(1)
N(2)–O(1)	2.957(6)	N(3A)–Ru–N(1)	171.9(1)
O(1)–O(2)	2.778(5)	N(3)–Ru–N(1)	96.5(1)
O(1)–O(2A)	2.862(5)	N(1)–Ru–N(1A)	75.4(2)

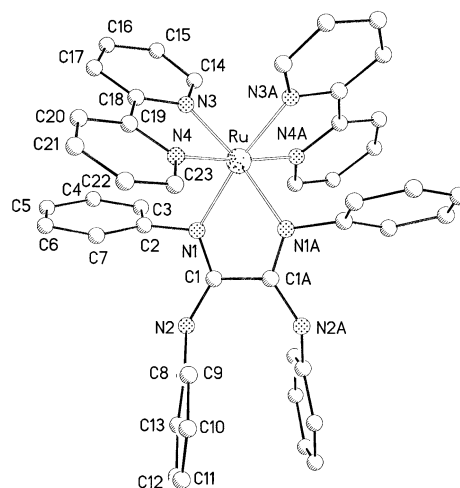


Fig. 5. Drawing of the X-ray structure of  $[(\text{bpy})_2\text{Ru}(\text{H}_2\text{TPOA})](\text{PF}_6)_2 \cdot 4\text{H}_2\text{O}$  (**1**) (anions and solvent molecules are omitted for reasons of clarity).

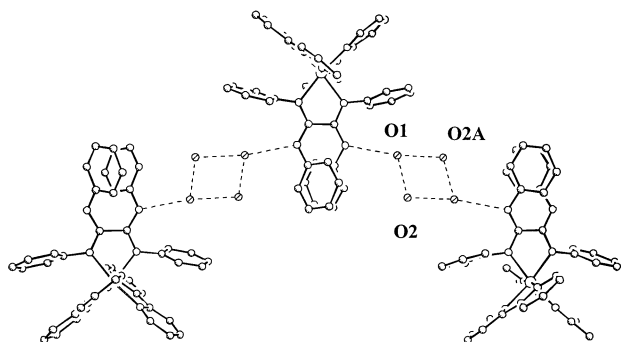


Fig. 6. Supramolecular structure of  $[(bpy)_2Ru(H_2TPOA)](PF_6)_2 \cdot 4H_2O$  (**1**) (anions are omitted for reasons of clarity).

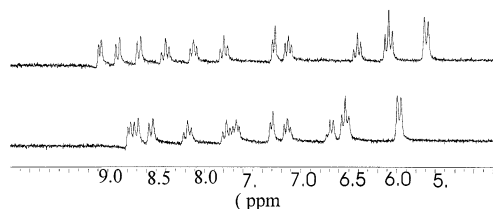


Fig. 7.  $^1H$  NMR spectra of the two diastereomers (**5'**) (above) and (**5''**) (below) in  $DMSO-d_6$  at 293 K.

complex cations whereby the cations are interconnected by the interaction of each N–H function with a planar ring consisting of four water molecules (see Fig. 6). The distance  $d_{N(H)-O} = 2.957(6)$  Å is in the typical range of H-bonding distances, while the distances between the oxygen atoms within in the planar water four ring are 2.778(5) and 2.957(5) Å. Thus, highly ordered solvent molecules create a supramolecular arrangement in the crystal.

It is worth mentioning that the position of the outward directed phenyl rings seems to suggest a  $\pi$ – $\pi$ -interaction. But compared with literature values [16], the distance of  $d_{phenyl-phenyl} = 3.78$  Å in the phenyl stacks indicates rather only simple crystal packing effects than  $\pi$ – $\pi$ -interaction as reason for this particular arrangement.

Table 2  
Absorption maxima and electrochemical data of the complexes **1–5** in acetonitrile <sup>a</sup>

Compound	$\lambda_{MLCT}$ (nm)	$\epsilon$ ( $l\text{ cm}^{-1}\text{ mol}^{-1}$ )	Ru(III/II) (V)	$pK_a$
$[Ru(bpy)_3]^{2+}$ [ <b>5</b> ]	452	$1.46 \times 10^4$	1.26	–
$[Ru(bpy)_2(H_2TPOA)]^{2+}$ ( <b>1</b> )	469	$1.39 \times 10^4$	0.94	9.19
$[Ru(Me-bpy)_2(H_2TPOA)]^{2+}$ ( <b>2</b> )	476	$1.17 \times 10^4$	0.90	9.33
$[Ru(bpy)_2(H_2TTOA)]^{2+}$ ( <b>3</b> )	472	$1.12 \times 10^4$	0.96	9.94
$[Ru(Me-bpy)_2(H_2TTOA)]^{2+}$ ( <b>4</b> )	478	$1.40 \times 10^4$	0.87	10.15
$\{[Ru(bpy)_2]_2(TPOA)\}^{2+}$ ( <b>5</b> )				
<b>5'</b>	520	(n.n.)	0.45/0.64	–
<b>5''</b>	526	(n.n.)	0.46/0.65	–

<sup>a</sup>  $pK_a$  values for **1–4**.

### 3.2. Synthesis and structure of the dinuclear compound $\{[Ru(bpy)_2]_2(TPOA)\}(PF_6)_2 \cdot 2H_2O$ (**5**)

The use of more than twofold excess of  $Ru(bpy)_2$ -precursor yields the dinuclear compound (**5**) in good yield. HPLC measurements indicate the presence of two compounds with a peak area of 50:50%. It was possible to separate these by recrystallisation in acetone–water (60/40 v/v%). Elemental analysis yielded identical compositions for both compounds and was indicative of a deprotonation of the tetraphenylloxalamidine ligand in both cases. The  $^1H$  spectra of the two fractions were recorded in  $DMSO-d_6$  and are depicted in Fig. 7. The spectra are only slightly different and exhibit a quite simple pattern with only one set of aromatic phenyl signals as expected for a high symmetrical complex. All peaks could be assigned unequivocally with the help of COSY experiments. No broad peaks, as in the mononuclear compounds, appear in the spectra and the phenyl rings of the  $TPOA^{2-}$  bridging ligand show only one well-resolved set of two triplets and one doublet. This suggests that in the dinuclear compound, the aryl rings are not free to rotate. The protons of the bipyridine ligands show the usual shifts and pattern.

On the basis of these observations, it seems reasonable to assume that the two fractions are optical isomers (**5'**) and (**5''**). The presence of stereoisomers is related to the well-known stereochemical problem of linking two metal ions with helical chirality by a bridging ligand [17]. This causes the emergence of one *meso*-form ( $\Delta\Delta$ ) and one enantiomeric pair with  $\Delta\Delta$  and  $\Lambda\Lambda$  configuration. The two isolated diastereomeric isomers (**5'**) and (**5''**) should correspond to the *meso*-( $\Delta\Delta$ )-compound and to the unresolved ( $\Delta\Delta/\Lambda\Lambda$ ) enantiomeric pair (enantiomers are indistinguishable in  $^1H$  NMR spectroscopy) [18], but with the data available it was not possible to assign the absolute configuration of (**5'**) and (**5''**).

### 3.3. Absorption spectra

The absorption spectra of compounds **1–5** were recorded in methanol–ethanol and show the typical

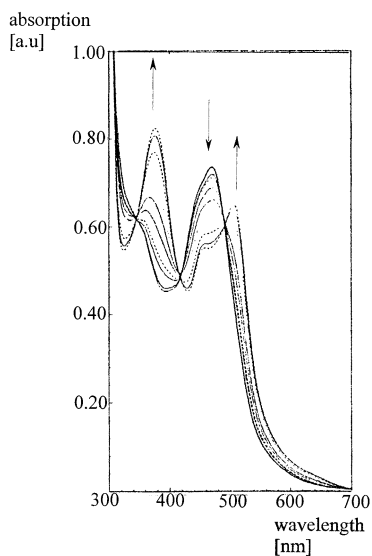


Fig. 8. pH-dependence of the absorption spectra of  $[\text{Ru}(\text{bpy})_2(\text{H}_2\text{TPOA})](\text{PF}_6)_2 \cdot 4\text{H}_2\text{O}$  (**1**) in the range from pH 3.08 to 12.05.

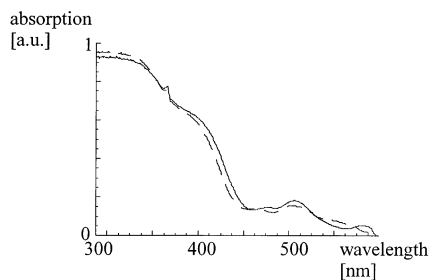


Fig. 9. UV-Vis spectra of compounds (**5**) (---) and (**5''**) (—).

features for members of the polypyridyl ruthenium(II) class. The results are summarised in Table 2. The most significant feature of these spectra is a strong band in the visible range due to  $d_{\pi-\pi^*}$ -MLCT transitions [19].

In comparison to the model compound  $[\text{Ru}(\text{bpy})_3]^{2+}$  ( $\lambda_{\text{MLCT}} = 452 \text{ nm}$ ), the MLCT bands of the oxalamidine complexes exhibit a shift to lower wavenumbers. Therefore, it can be suggested that the investigated oxalamidines possess stronger  $\sigma$ -donor and weaker  $\pi$ -acceptor properties than bipyridine. The presence of methylsubstituents in compounds **2** and **4** has only a minor influence on the absorption maxima. The MLCT-maximum of the dinuclear compound is observed at a lower energy than in the monomeric compounds. This reflects the deprotonation of the bridging ligand and it is indicative of the stronger  $\sigma$ -donor and weakened  $\pi$ -acceptor properties of the deprotonated bridge.

The possibility of tuning the absorption spectra of the compounds **1–4** by changing the acidity of the solution was investigated. Thus, Fig. 8 shows the absorption spectra of compound **1** in the range from pH

3.08 to 12.05. In this range, only one set of isobestic points is found. The MLCT band around  $\lambda = 470 \text{ nm}$  collapses gradually upon deprotonation and two new bands appear. The emerging band at  $\lambda = 505 \text{ nm}$  can be assigned to a MLCT transition in the deprotonated complex. The deprotonated tetraphenylloxalamidine ligand should act as a stronger  $\sigma$ -donor and increasing electron density around the metal shifts the maximum of the MLCT band to higher wavelengths. The band at  $\lambda = 380 \text{ nm}$  might correspond to an additional MLCT band to either bpy or to  $\text{H}_2\text{TPOA}$ .

From the absorption spectra it was possible to determine the  $\text{p}K_{\text{a}}$  values for compounds **1–4** (see Table 2). The  $\text{p}K_{\text{a}}$  is relatively insensitive to substitution changes on both the bpy ligand and the oxalamidines. Only one protonation step could be observed in the range measured for all complexes. This might suggest that both N–H functions are deprotonated at the same time or that the second deprotonation is outside the range measured.

The two diastereomers (**5'**) and (**5''**) show slightly different absorption spectra (see Fig. 9). Potential differences in the electronic behaviour of diastereomeric and enantiomeric isomers of polypyridyl ruthenium(II) complexes were the subject of several recent investigations [20,21]. Multinuclear ruthenium polypyridyl complexes will normally contain a manifold of diastereomers and these studies are aimed at determining whether optical isomers have significantly different photophysical properties. That is a rather important problem, because constructing antenna systems from Ru–bipyridyl units demands the very strict control of the photophysical properties of such light absorbing devices.

Surprisingly, the measurement of compounds **1–5** does not show any emission. Even cooling down to 77 K in various solvents and extended change of the pH-value did not render the expected emission. This is an unexpected result, because the appearance of an emission from a long living  $^3\text{MLCT}$  state is to be seen as one of the intrinsic characteristics for polypyridyl–Ru(II) compounds. One possible explanation might be that the electron occupies an oxalamidine  $\pi^*$ -orbital instead of a bpy  $\pi^*$ -orbital in the excited state. Thus, the inappropriateness of the oxalamidine  $\pi^*$ -orbitals to deliver a long living excited state could explain the absence of emission. This assumption might be supported by the first reduction potentials for compounds **1–4** which are irreversible, in contrast to those of polypyridyl–Ru(II) complexes.

### 3.4. Electrochemistry

The Ru(III)/(II) potentials for the  $\text{PF}_6^-$ -salts in 0.1 M solution of tetra-*n*-butylammonium perchlorate in acetonitrile versus saturated calomel electrode are sum-

marised in Table 2. In comparison with  $[\text{Ru}(\text{bpy})_3]^{2+}$  ( $E_{\text{III/II}} = 1.23$  V vs. SCE) all redox Ru(III/II) couples of the mononuclear complexes **1–4** are shifted to more negative potentials ( $E_{\text{III/II}} = 0.96\text{--}0.87$  V), in agreement with an increased electron density around the ruthenium ion caused by the better  $\sigma$ -donor properties of the oxalamidine ligands. Methyl substitution on the bipyridine ligands pushes the Ru(III/II) couples to somewhat more negative potentials, consistent with the results of absorption measurements described before. Substitution at the oxalamidine does not significantly affect the oxidation couple. The oxidation potentials for the two isomers of the dimeric compound **5** differ only slightly. The oxidation of the dinuclear complexes results in two one electron single waves, which are separated by 190 mV for both isomers. Using this value the comproportionation constant  $K_{\text{com}}$  for **5** was calculated following the relationship (at  $T = 298$  K) [22]

$$K_{\text{com}} = \exp\{\Delta E(\text{mV})/25.69\} = 1.63 \times 10^3$$

This value points to a substantial electronic interaction between the two metal centres. The oxidation of the first centre causes an increase in the charge of the complex and therefore the second oxidation occurs at a higher potential. In compound **5** the first oxidation couple occurs at  $E_{\text{III/II}} = 0.45\text{--}0.46$  V exhibiting the strong  $\sigma$ -donor capability of the deprotonated bridging ligand. Thus, the second oxidation occurs at a more negative potential ( $E_{\text{III/II}} = 0.64/0.65$  V) than the lowest of the mononuclear compounds, for which the oxidation potential is found at about 0.90 V. This is most likely explained by the double negative charge on the bridging ligand.

#### 4. Conclusions

We have prepared a series of novel mononuclear complexes of the type  $[\text{Ru}(\text{bpy})_2(\text{LL})]^{2+}$  with LL =  $\text{H}_2\text{TPOA}$ ,  $\text{H}_2\text{TTOA}$  as members of a new class of non aromatic 1,2-diimine ligands in polypyridyl ruthenium(II) chemistry. The structure of the mononuclear compounds was elucidated by  $^1\text{H}$  NMR, FAB MS and X-ray investigations. The coordination of the  $\text{Ru}(\text{bpy})_2$ -moiety to the 1,2-diimine unit was assured unambiguously by X-ray structure determination of compound  $[\text{Ru}(\text{bpy})_2(\text{H}_2\text{TPOA})](\text{PF}_6)_2 \cdot 4\text{H}_2\text{O}$  (**1**). On supramolecular level, complex **1** forms chainlike structures, whereby the complex cations are interconnected via their N–H functions by four ordered water molecules. Surprisingly, the complexes **1–5** do not exhibit any emission under any condition. The dinuclear compound  $\{[\text{Ru}(\text{bpy})_2]_2\text{TPOA}\}(\text{PF}_6)_2 \cdot 2\text{H}_2\text{O}$  (**5**) was prepared and structurally characterised. We succeeded in separating the two diastereomers by recrystallisation and could confirm small but significant differences in electronic spectra.

Finally we propose that since they possess potential for H-bonding and intercalation by  $\pi$ -stacking with biological substrates (e.g. DNA), the mononuclear complexes **1–4** can become valuable building blocks in supramolecular architectures. Future research efforts will follow this line.

#### 5. Supplementary material

Further details of the crystal investigations are available on requests from the Director, Cambridge Crystallographic Data Centre, 12 Union Road, Cambridge CB2 1EZ, UK, on quoting the depository number CCDC 13099, the names of the authors, and the journal citation.

#### Acknowledgements

We would like to thank to Professor U.-W. Grummt and Mrs E. Backhaus for collaboration in some experiments and for measuring several spectra. This work was supported financially by the Studienstiftung des deutschen Volkes by a doctoral scholarship for M. Ruben and S. Rau and by the Deutsche Forschungsgemeinschaft (SFB 436).

#### References

- [1] (a) J.-P. Collin, P. Gavina, P. Heitz, J.-P. Sauvage, *Eur. J. Inorg. Chem.* 1 (1998) 1. (b) A. Livoreil, J.-P. Sauvage, N. Armaroli, V. Balzani, L. Flamigni, B. Ventura, *J. Am. Chem. Soc.* 119 (1997) 12114. (c) V. Balzani, A. Juris, M. Venturi, S. Campagna, S. Serroni, *Chem. Rev.* 96 (1996) 759.
- [2] (a) R.E. Holmlin, P.J. Dadliker, J.K. Barton, *Angew. Chem., Int. Ed. Engl.* 36 (1997) 2714. (b) A. Magnuson, Y. Frapart, M. Abrahamson, O. Horner, B. Åckermark, L. Sun, J.-J. Girerd, L. Hammarström, S. Styring, *J. Am. Chem. Soc.* 121 (1999) 89.
- [3] J.-P. Sauvage, J.-P. Collin, J.-C. Chambron, S. Guillerez, C. Coudret, V. Balzani, F. Barigelletti, L. DeCola, L. Flamigni, *Chem. Rev.* 94 (1994) 993.
- [4] J.A. Bolger, G. Ferguson, J.P. James, C. Long, P. McArdle, J.G. Vos, *J. Chem. Soc., Dalton Trans.* (1993) 1577.
- [5] A. Juris, V. Balzani, F. Barigelletti, S. Campagna, P. Belser, A.v. Zelewsky, *Coord. Chem. Rev.* 84 (1988) 85.
- [6] M. Döring, H. Görls, R. Beckert, *Z. Anorg. Allg. Chem.* 620 (1994) 551.
- [7] J. Trofimenko, *J. Am. Chem. Soc.* 89 (1967) 7014.
- [8] E. Papafil, A. Papafil, A. Kleinstein, I. Gabe, V. Macovei, *Analele Stiint. Univ. 'Al. I. Cuza' Iasi, Sect. I* 10c (1964) 115.
- [9] D. Lindauer, R. Beckert, M. Döring, P. Fehling, H. Goerls, *J. Prakt. Chem.* 337 (1995) 143.
- [10] K. Bauer, *Chem. Ber.* 40 (1907) 2655.
- [11] (a) R. Hage, J.G. Haasnoot, J. Reedijk, R. Wang, J.G. Vos, *Inorg. Chem.* 30 (1991) 3263. (b) R. Hage, *Coord. Chem. Rev.* 111 (1991) 161.
- [12] S. Vorwerk, Diploma thesis, Friedrich-Schiller-University, Jena, 1992.

- [13] Z. Otwinowski, W. Minor, Processing of X-ray diffraction data collected in oscillation mode, in *Methods in Enzymology*, in: C.W. Carter, R.M. Sweet (Eds.), *Macromolecular Crystallography, Part A*, vol. 276, Academic, London, 1997, pp. 307–326.
- [14] G.M. Sheldrick, *Acta Crystallogr., Sect. A* 46 (1990) 467.
- [15] G.M. Sheldrick, SHELXL-97, University of Göttingen, Germany, 1993.
- [16] C.A. Hunter, J.K.M. Sanders, *J. Am. Chem. Soc.* 112 (1990) 5525.
- [17] A. von Zelewsky, *Chimia* 48 (1993) 331.
- [18] B. Testa, *Grundlagen der Organischen Stereochemie*, Verlag Chemie, Weinheim, 1983, p. 158.
- [19] K. Kalanyasundaram, *Photochemistry of Polypyridine and Porphyrin Complexes*, Academic, London, 1992.
- [20] (a) X. Hua, A.v. Zelewsky, *Inorg. Chem.* 30 (1991) 3796. (b) K. Wärnmark, J. Thomas, O. Heyke, J.-M. Lehn, *J. Chem. Soc., Chem. Commun.* (1994) 2075. (c) F.R. Keene, *Coord. Chem. Rev.* 166 (1997) 121. (d) F.R. Keene, *Chem. Soc. Rev.* 27 (1998) 185.
- [21] (a) S. Serroni, G. Denti, S. Campagna, M. Ciano, V. Balzani, *J. Am. Chem. Soc.* 114 (1992) 2944. (b) S. Serroni, G. Denti, S. Campagna, A. Juris, M. Ciano, V. Balzani, *Angew. Chem., Int. Ed. Engl.* 31 (1992) 1493. (c) T.J. Rutherford, O. Van Gijte, A. Kirsch-De Mesmaker, F.R. Keene, *Inorg. Chem.* 36 (1997) 4465.
- [22] G. Giuffrida, S. Campagna, *Coord. Chem. Rev.* 135/136 (1994) 517.